Journal of Inorganic and General Chemistry
ZAAC
Zeitschrift für anorganische und allgemeine Chemie
www.zaac.wiley-vch.de
RESEARCH ARTICLE
Check for updates
DOI: 10.1002/zaac.202400135

Supramolecular Interactions as Key in Racemic Resolution: New Insights into the (S_{Si})- and (R_{Si})-Diastereomers of (1*R*,2*S*,5*R*)-Methyl(1-naphthyl)-phenylmenthoxysilane of *Sommer*

Jan-Lukas Kirchhoff[a] and Carsten Strohmann*[a]

A highly selective approach with high yields of two diastereomeric silicon-stereogenic menthoxysilanes, (R_{Si})-**3** and (S_{Si})-**3**, introduced by *Sommer et al.*, could be established as well as investigated in detail using different analytical tools. Single-crystal X-ray diffraction analysis was used to examine the different crystallization rates while *Hirshfeld* surface analysis was applied to extend supramolecular interactions in the solid state which showed stronger hydrogen bridges for the faster crystallizing diastereomer (S_{Si})-**3**. In addition, similar ground-state energies haven been found for both diastereomers by DFT calculations. Subsequent NMR studies showed stable Si-configurations wherein epimerization only started after more than 4 hours at 110 °C. Access to both diastereomers with opposite configuration at the stereogenic silicon center is achievable in high yields and high stereochemical purity using only naturally occurring (–)-menthol as a reagent.

Introduction

Silicon-stereogenic compounds play a pivotal role in chemistry, as they can serve as stereogenic probes,[1] chiral reagents,[2] or for the creation of carbon-centered chirality in organic synthesis, such as in hydrosilylation reactions.[3] However, access to stereochemically pure organosilanes has been limited and was not extensively explored until the late 1950s by pioneers such as *Sommer*[4,5] and *Corriu*.[6] Initially, chiral silicon compounds were obtained through racemic resolution or enzymatic esterification.[7] Over the following years, the induction of a stereogenic center at the silicon atom has been continuously investigated. Notable methods include asymmetric syntheses via substrate or reagent induction,[8] which our research group has further expanded with several examples.[9] Additional approaches for synthesizing Si-stereogenic compounds involve chiral silyl anions,[10] with recent developments in catalytic methods also producing highly pure compounds.[11] These chiral catalysts often require extensive multi-step synthesis and are costly. Furthermore, these stereospecific reactions consistently produce enantiomers or diastereomers with a fixed configuration at the silicon center, dependent on the absolute configuration of the corresponding reagent or catalyst. Despite highly selective approaches to such Si-stereogenic compounds, the absolute configuration at the silicon center depends on the chiral auxiliary used, meaning that two different chiral auxiliaries are always required for (S_{Si})- and (R_{Si})-configured products. In kinetic racemate resolutions, it is common that one diastereomer can be enriched better, e.g. by fractional crystallization, and therefore one is used more frequently. The diastereomer remaining in solution is usually more difficult to purify and is rarely used in preparative synthesis, as the following example shows.

A very important key racemic resolution in silicon chemistry was established by *Sommer et al.*, which enables access to two Si-stereogenic diastereomers *via* fractional crystallization.[4]

Starting with commercially available phenylmethyl-dimethoxysilane (**1**), a 1-naphthyl group is introduced at the silicon center *via* a substituion reaction by a *Grignard* reagent[12] using 1-naphthyl bromide. The resulting racemic methoxysilane (*rac*-**2**) can then be converted into a mixture of diastereomers through a substitution reaction *via* (–)-menthol under basic conditions (see Scheme 1).

These two diastereomers, (S_{Si},1R_C,2S_C,5R_C)-**3** and (R_{Si},1R_C,2S_C,5R_C)-**3**, are historically central silicon-stereogenic compounds for stereospecific syntheses in silicon chemistry. Since only the absolute configuration of the stereogenic silicon atom is changed for the further work and all other configurations at the menthoxy group are not affected, (S_{Si},1R_C,2S_C,5R_C)-**3** is referred as (S_{Si})-**3** and (R_{Si},1R_C,2S_C,5R_C)-**3** as (R_{Si})-**3**. *Sommer et al.* successfully analyzed both diastereomers, noting differences in specific rotations and melting points. In this process, the higher melting diastereomer, which was later assigned the (S_{Si})-configuration, always crystallized first in *n*-petane, whereby the low-melting (R_{Si})-configurated diastereomer was obtained after multiple recrystallization in ethanol. The diastereomeric purity could not be determined by a direct measurement method. The subsequent chemistry in stereo-

[a] *J.-L. Kirchhoff, C. Strohmann*
Institute of Inorganic Chemistry, TU Dortmund University, Otto-Hahn-Str. 6, 44227 Dortmund, Germany
E-mail: carsten.strohmann@tu-dortmund.de

Supporting information for this article is available on the WWW under https://doi.org/10.1002/zaac.202400135

Journal of Inorganic and General Chemistry
ZAAC
Zeitschrift für anorganische und allgemeine Chemie

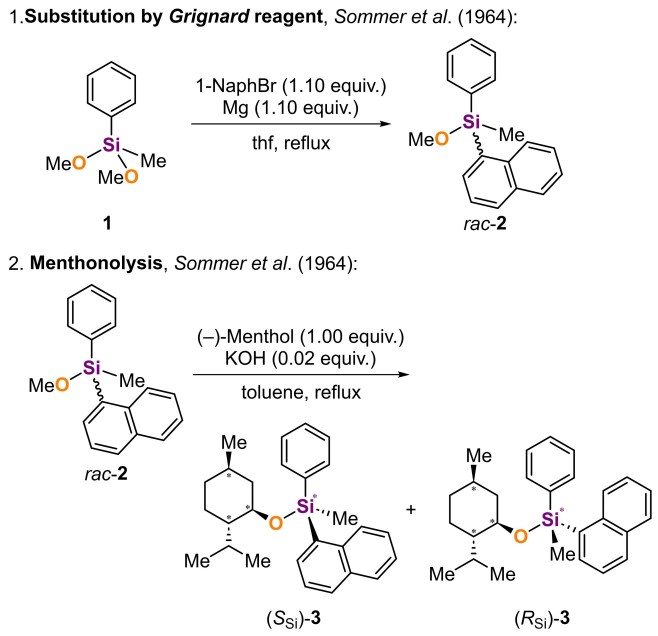

Scheme 1. Top: Substitution of the *in situ* generated *Grignard* 1-naphthylmagnesium bromide to the racemic methoxysilane *rac*-**2**. Bottom: Subsequent reaction *via* alcoholysis with (–)-menthol under basic conditions to synthesize both diastereomers (S_{Si})-**3** and (R_{Si})-**3** in the mother liquor.

specific syntheses shows that (S_{Si})-**3** could be obtained with very high stereochemical purity. However, documentation of both diastereomers is not available with complete characterization, which is in particular due to the poorer accessibility of (R_{Si})-**3** because of its decreased crystallization properties. Diastereomerically and enantiomerically pure menthoxysilanes serve as suitable precursors for the synthesis of enantiomerically pure monohydrosilanes, which can be obtained stereochemically selective and in good yields via reduction reactions.[4,13]

In this work, we present a selective approach to both diastereomers and aim to investigate the different crystallization behaviors of the two diastereomers using modern analytical methods. In particular, we intend to utilize single-crystal X-ray diffraction analysis, which can detect the smallest differences in their respective solid-state structures and could explain the crystallization occurrence.

Results and Discussion

For the synthesis of diastereomeric mixture (S_{Si})-**3** and (R_{Si})-**3**, the literature-known synthesis was performed, starting from phenylmethyldimethoxysilane (**1**) to the racemic methoxysilane *rac*-**2** and finally synthesizing menthoxysilanes (S_{Si})-**3** and (R_{Si})-**3** *via* alcoholysis.[4]

Here, we were able to crystallize and fully characterize both diastereomers with high yields and excellent stereochemical purities with a different approach than *Sommer et al.* In *n*-pentane, the (S_{Si})-configured diastereomer consistently crystallized first. We have verified the stereochemical purity of *d.r.* ≥ 99:1 as confirmed by NMR spectroscopy. The absolute configuration at the stereogenic silicon center was determined relative to the enantiomerically pure (–)-menthoxy group and further confirmed via the *Flack* parameter [(–0.015(10)][14] (see Figure 1).

For the structural refinement of the measurement data, besides the typical spherical atomic form factors (*SHELX*), *NoSpherA2*[15] was also used as a different model for the description of the X-ray experiment. This structure refinement method uses non-spherical atom form factors. Each atom is assigned custom atom scattering factors, which again can be obtained from the electron density. For this purpose, *NoSpherA2* uses quantum mechanical calculations, e.g. DFT calculations, enabling much more precise structure refinements and much more accurate standard deviations. The structures we have obtained, provide the high data quality necessary to make this method even more precise. For all significant bond lengths and bond angles, the corresponding *NoSpherA2* values are given in square brackets. The menthoxysilane (S_{Si})-**3** exhibits a slightly distorted tetrahedral structure at the silicon center, which can be explained by the large methoxy substituent. This steric hindrance results in angles of C1–Si1–O1 = 106.21(3)° [106.300(6)°][16] and C27–Si1–O1 = 111.43(3)° [111.420(5)°].[16] An important observation is the increased angle C17–O1–Si1 = 126.45(3)° [126.577(4)°][16] at the oxygen atom, which could indicate a significant effect in the crystal. Si–C- and Si–O-bonds are comparable to those in analogous structures and do not exhibit any peculiarities.[17]

However, it remains to be determined how the solid-state structure of the other diastereomer (R_{Si})-**3** appears and how it

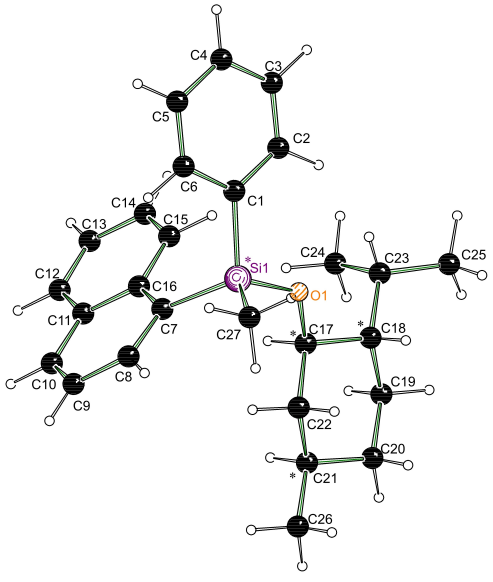

Figure 1. Molecular structure of (S_{Si})-**3** in the solid-state with selected bond lengths [Å] and angles [°]. Si1–O1 1.6470(4), Si1–C1 1.8731(5), Si1–C7 1.8819(6), Si1–C27 1.8686(7), O1–C17 1.4414(6); C1–Si1–O1 106.22(2), C27–Si1–O1 111.43(3), C1–Si1–C7 110.69(2), C17–O1–Si1 126.45(3); CCDC deposition number: 2363296.

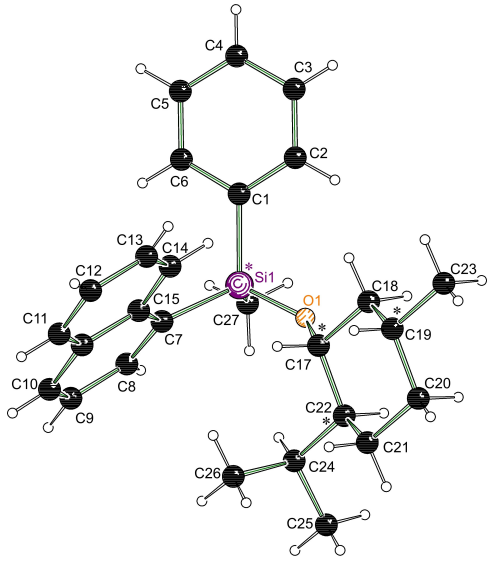

Figure 2. Molecular structure of (R_{Si})-**3** in the solid-state with selected bond lengths [Å] and angles [°]. Si1–O1 1.6371(4), Si1–C1 1.8719(5), Si1–C7 1.8797(6), Si1–C27 1.8620(7), O1–C17 1.4337(6); C1–Si1–O1 111.48(3), C27–Si1–O1 104.08(3), C1–Si1–C7 110.52(2), C17–O1–Si1 132.85(4); CCDC deposition number: 2363300.

compares to the (S_{Si})-configured compound. To investigate this question, (R_{Si})-**3** was initially isolated and fully characterized afterwards.

After separating the (S_{Si})-diastereomer, the mother liquor was dissolved in diethyl ether, a slightly more polar solvent, unlike *Sommer et al.* who used ethanol and stored at −30 °C afterwards. The resulting crystals subsequently contained the (R_{Si})-configured diastereomer, which was verified by single-crystal X-ray structural analysis (see Figure 2). Once again, we have verified the stereochemical purity of *d.r.* ≥ 99:1 as confirmed by NMR spectroscopy The absolute configuration at the stereogenic silicon center was determined relative to the enantiomerically pure (–)-menthoxy group and further confirmed via the *Flack* parameter [−0.018(9)].[14]

Once again, a distorted tetrahedral structure with altered tetrahedral angles at the silicon center was observed, whereas the bond lengths are comparable to those in the structure of (S_{Si})-**3**. However, there is an opposite effect observed in the distorted angles, as they now measure C1–Si1–O1 = 111.48(3)° [111.468(3)°][16] and C27–Si1–O1 = 104.09(3)° [104.1579(12)°].[16] A significant difference can be seen in the increased angle at the oxygen atom C17–O1–Si1 = 132.85(4)° [133.0080(16)°],[16] which is approx. 6° larger than in (S_{Si})-**3**. This structural difference in both diastereomers is most likely due to packing effects in the crystal, which will be analysed next Table 1.

One possible explanation could be the diverse supramolecular interactions of the two compounds in the

Table 1. Important crystal and structure refinement data for (S_{Si})-**3** (CCDC deposition number: 2363296; NoSpherA2 refined structure: 2367654) and (R_{Si})-**3** (CCDC deposition number: NoSpherA2 refined structure: 2367642).

	(S_{Si})-**3**	(R_{Si})-**3**
Empirical formula	$C_{27}H_{34}OSi$	$C_{27}H_{34}OSi$
Formula weight/g mol^{-1}	402.63	402.63
Temperature/K	100	100
Crystal system	monoclinic	trigonal
Space group	$P2_1$	$P3_2$
a/Å	9.1459(8)	9.3666(3)
b/Å	15.2650(12)	9.3666(3)
c/Å	9.3230(9)	23.0403(10)
α/°	90	90
β/°	116.113(3)	90
γ/°	90	120
Cell volume/Å^3	1168.75(18)	1750.58(14)
Z	2	3
ρ_{calc}/g cm^{-3}	1.144	1.146
Absorption coefficient ***μ***/mm^{-1}	0.115	0.116
F(000)	436.0	654.0
Size of crystal/mm^3	1.143×0.912×0.318	0.761×0.648×0.417
Radiation	MoK_α (λ = 0.71073)	MoK_α (λ = 0.71073)
2Θ-Area for data collection/°	4.866–88.528	5.022–90.606
Index area	$-17 \le h \le 17$, $-29 \le k \le 29$, $-18 \le l \le 18$	$-18 \le h \le 18$, $-18 \le k \le 18$, $-46 \le l \le 46$
Collected reflexes	644113	436699
Independent reflexes	18478 [R_{int} = 0.0546, R_{sigma} = 0.0125]	19575 [R_{int} = 0.0480, R_{sigma} = 0.0144]
Data/Restraints/Parameter	18478/1/398 [568][16]	19575/1/398 [568][16]
Goodness-of-fit on F^2	1.052 [1.198][16]	1.063 [1.111][16]
Final *R*-value [$I \ge 2\sigma$ (*I*)]	R_1 = 0.0272 [0.0168],[16] wR_2 = 0.0752 [0.0355][16]	R_1 = 0.0284 [0.0178],[16] wR_2 = 0.0737 [0.0283][16]
Final *R*-value [all Data]	R_1 = 0.0287 [0.0183],[16] wR_2 = 0.0770 [0.0363][16]	R_1 = 0.0316 [0.0211],[16] wR_2 = 0.0758 [0.0290][16]
Rest electron density/e Å^{-3}	0.49/−0.14 [0.35/−0.11][16]	0.43/−0.16 [0.23/−0.12][16]
***Flack* parameter**[14]	−0.015(10) [0.000(6)][16]	−0.018(9) [0.017(8)][16]

crystalline solid state, which might also account for the significantly different melting points of the diastereomers as reported by *Sommer et al.* However, diastereomeric purity could not be determined by a direct measurement method. A comparison of the melting points of the isolated compounds from the studies of *Sommer et al.* and the stereochemically pure compounds from this work shows that the melting point of (S_{Si})-**3** is almost identical. However, our melting point of (R_{Si})-**3** is approximately 5 °C higher according to *Sommer et al.* This may be explained by impurities or a lower diastereomeric purity in the studies by *Sommer et al.*

That observation also suggests that there should be significant changes in the packing structure of both crystalline diastereomers that could explain the different properties.

For a more in-depth analysis, a *Hirshfeld* analysis[18] was performed using *Crystal Explorer v.21.5*[19] to visualize the intermolecular interactions (see Figure 3).

The Hirshfeld surface of (S_{Si})-**3** reveals several C–H···O contacts highlighted in red on the surface. Particularly notable is the hydrogen bond C12–H12···O1, which facilitates strong intermolecular interactions within the solid state. The length of this contact is H12–O1 = 2.550(16) Å [2.4373(2) Å][16] and C12···O1 = 3.4787(7) Å [3.4779(3) Å].[16] The angle C12–H12–O1 = 170.7(14)° [171.4967(7)°][16] indicates an exceptionally strong hydrogen bond of the C–H···O type. This is also evident from the corresponding fingerprint plots, which show prominent peaks in the two-dimensional diagram. It is further observed that the stronger contacts are due to O···H/H···O and H···H interactions.

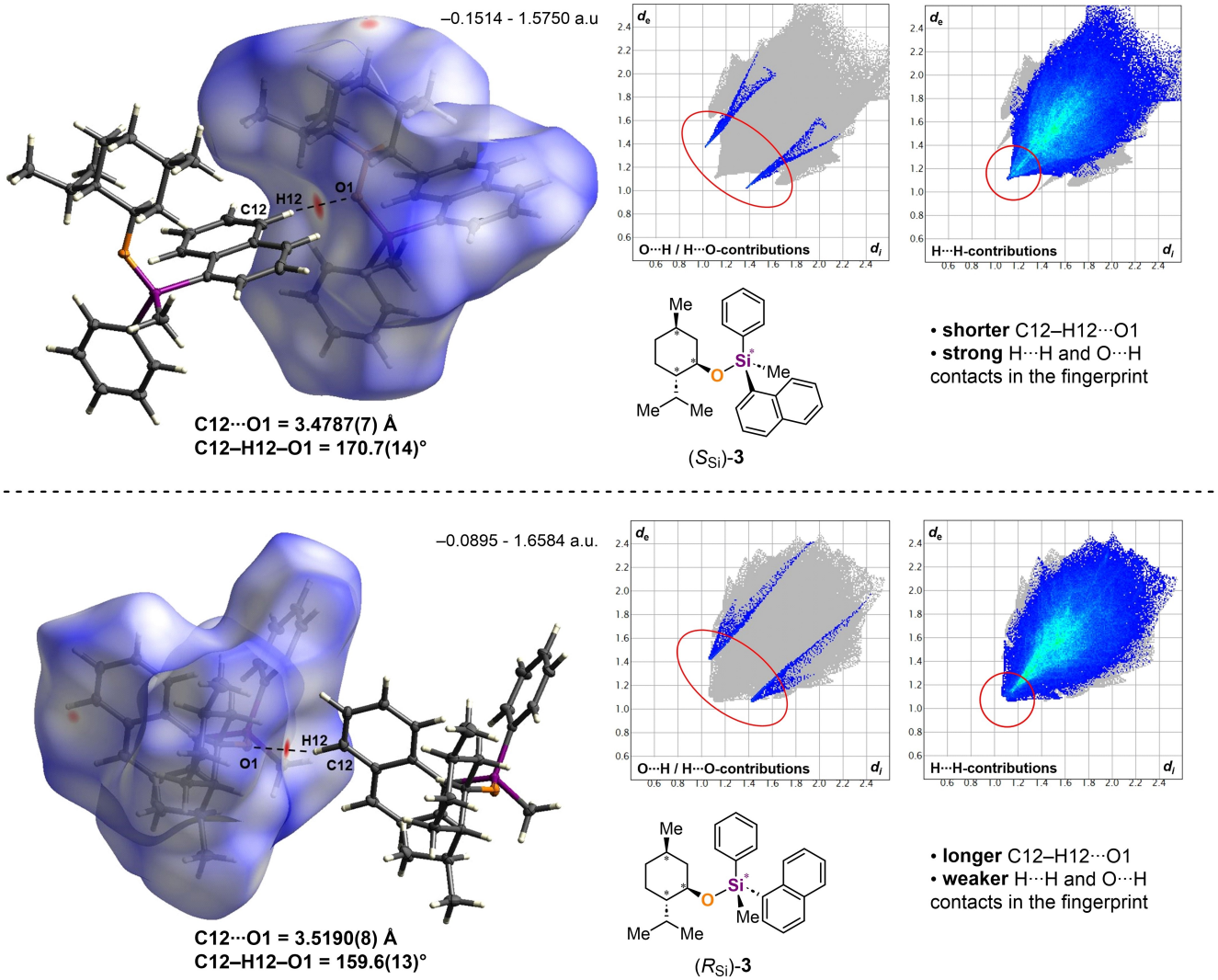

Figure 3. *Hirshfeld* analyses and fingerprint plots of the two diastereomers (S_{Si})-**3** and (R_{Si})-**3**. The *Hirshfeld* surfaces were generated from the structurally refined data using IAM, without NoSpherA2. Top: *Hirshfeld* surface of (S_{Si})-**3**, highlighting the hydrogen bond C12–H12···O1 (−0.1514–1.5750 a.u.). The red ellipse or circle in the two fingerprint plots emphasizes the strong supramolecular interactions in comparison. Bottom: *Hirshfeld* surface of (R_{Si})-**3**, also highlighting the hydrogen bond C12–H12···O1 (−0.0895–1.6584 a.u.). The red ellipse and circle in the two fingerprint plots emphasize the weaker supramolecular interactions in comparison. to (S_{Si})-**3**.

Similar to this procedure, the *Hirshfeld* surface of (R_{Si})-**3** was visualized using *Crystal Explorer v.21.5* and compared with the surface properties of (S_{Si})-**3**.

Upon analysis of (S_{Si})-**3**, it becomes evident that the hydrogen bond C12–H12···O1 represents a pronounced intermolecular interaction once again. However, due to the molecule's orientation in the cell and the configuration at the silicon center, this interaction is noticeably weaker. Now, the bond lengths of the contacts H12–O1 = 2.646(17) Å [2.49915(9) Å][16] and C12···O1 = 3.5190(8) Å [3.51926(12) Å][16] are significantly longer. The angle C12–H12···O1 = 159.6(13)° [157.8369(11)°][16] is also significantly smaller compared to (S_{Si})-**3**. The difference of the angles ensures a more pronounced hydrogen bonding in (S_{Si})-**3** with increased higher linearity. This difference is also observed in the corresponding two-dimensional fingerprint plots, where the peaks indicating strong contacts are comparatively weaker.

This observation may provide a reason for the lower melting point of (R_{Si})-**3** (T_{mp} = 62.5 °C) compared to (S_{Si})-**3** (T_{mp} = 82.5 °C).

Next, the molecular geometries of both diastereomers without packing effects in the gas phase were determined using DFT calculations to verify whether packing in the crystal also affects bond lengths and angles. In particular, the angle at the oxygen atom, C17–O1–Si1, was analyzed and compared with the structural data. In addition, these calculations aim to quantify the ground-state energy difference of both diastereomers based on their respective energies.

Both molecules were optimized using the quantum chemical level M062x/6-311 + G(d,p). The ground-state energies differ by less than 1 kJ mol^{-1}, which is within the systematic error range of quantum chemical methods. This suggests that neither diastereomer should be significantly more energetically stable than the other under these computational conditions, although solvent or solid-state effects were not explicitly considered in the gas-phase calculations (see Figure 4).

Besides investigating the different gas phase ground state energies, it is important to investigate the C17–O1–Si1 angle. The data shows that the angles have a similar size. The angle for (S_{Si})-**3** is C17–O1–Si1 = 127.52°, the corresponding angle for (R_{Si})-**3** is C17–O1–Si1 = 129.85° [M062x/6-311 + G(d,p)]. Although the DFT calculations confirm the trend that the angle for the (R_{Si})-configured diastereomer is larger, these calculations cannot describe the large structural difference in the solid state structure of 6.4° [C17–O1–Si1 = 126.45(3)° in (S_{Si})-**3**; C17–O1–Si1 = 132.85(4)° in (R_{Si})-**3**.

Up until this point, it can be concluded that the supramolecular analysis can explain the different crystallization rates, which are further reflected in the distinct melting temperatures of the diastereomers. Access to both diastereomers is achievable in high yields and high stereochemical purity using only naturally occurring (–)-menthol as a reagent. An important subsequent question regarding both molecules is whether the stereogenic information at the silicon center remains stable under various reaction conditions.

To address this question, NMR studies were conducted. The stereochemically pure (R_{Si})-diastereomer (R_{Si})-**3** was dissolved in toluene-d_8, refluxed for 16 hours, and subsequently analyzed by

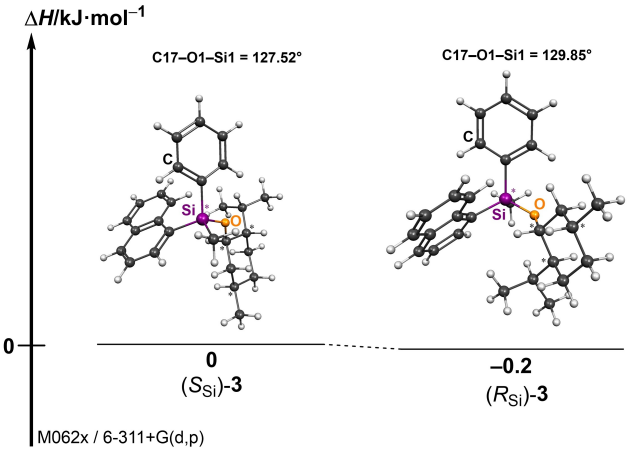

Figure 4. Comparison of enthalpies H [kJ mol^{-1}] of the two diastereomers (S_{Si})-**3** and (R_{Si})-**3** determined by DFT calculations. The absolute enthalpy of the (S_{Si})-configured diastereomer was referenced to 0 kJ mol^{-1} to illustrate the energy difference with the other diastereomer. Quantum chemical level: M062x/6-311 + G(d,p), calculations performed in the gas phase.

NMR spectroscopy. The ^{29}Si NMR spectrum, in which both diastereomers are baseline-separated, shows only the corresponding peak of (R_{Si})-**3**. No epimerization can be observed. The same solution in the same NMR tube was then exposed for additional 4 hours after addition of one equivalent of KOH and (–)-menthol, and reanalyzed by NMR spectroscopy for the diastereomeric ratio. It was found that there is small loss of stereochemical information at the silicon center. However, this observation changes significantly if the reaction solutions are heated for another 72 hours. During this time, epimerization can be observed, as evidenced by the recorded ^{29}Si NMR spectrum. The diastereomeric ratio is *d.r.* = 52:48 (see Figure 5). These NMR studies represent initial investigations into the configurational stability of the diastereomers (S_{Si})-**3** and (R_{Si})-**3**. In these studies, the precise mechanistic principles of epimerization with other alcohols under harsh conditions need further investigations. However, it can already be verified after these experiments that the configurations at the silicon center are stable in solution and even at reaction temperatures up to 110 °C.

Conclusions

A detailed analysis on the simple accessible synthesis of two Si-stereogenic diastereomers was carried out, both diastereomers were fully characterized using various analytical tools. The diastereomers, (S_{Si})-**3** and (R_{Si})-**3**, were structurally examined *via* single-crystal X-ray diffraction analysis, the stereochemical purity was confirmed by NMR spectroscopy. Based on the structural differences in the solid state and the stronger supramolecular interactions in (S_{Si})-**3**, which can be proven by stronger hydrogen bonding. A likely reason for the differing crystallization rates was elucidated, which was previously

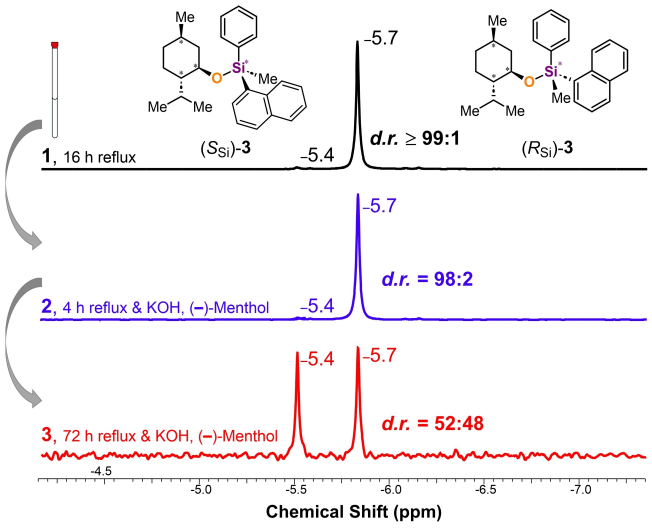

Figure 5. NMR study to verify the stability of the stereogenic silicon center of (R_{Si})-**3**: Displayed are three ^{29}Si NMR spectra of the pure diastereomer (R_{Si})-**3** dissolved in toluene-d_8. The diastereomeric ratio *d.r.* refers to the ratio (R_{Si})-**3** to (S_S)-**3**. The first ^{29}Si NMR spectrum was recorded after 16 hours of heating under reflux (**1**). The second ^{29}Si NMR spectrum was obtained after the addition of KOH and (–)-menthol, followed by an additional 4 hours of heating under reflux (**2**). The third ^{29}Si NMR spectrum was taken after a further 72 hours of heating under reflux (**3**). The NMR spectra were recorded sequentially using the same sample.

suggested by the different melting points of the two diastereomers.

This two-step synthesis starting from the commercially available dimethoxysilane **1**, including fractional crystallization, only needs to be carried out once to obtain both stereochemically pure diastereomers. Additionally, it was demonstrated that the configuration at the silicon center remains stable even at higher reaction temperatures, with no epimerization of the compounds.

Access to both diastereomers with opposite configuration at the stereogenic silicon center is achievable in high yields and high stereochemical purity using only naturally occurring (–)-menthol as a reagent.

Experimental Section

General Considerations

All reactions were performed in standard glass apparatuses with undried solvents. Unless otherwise stated, commercially purchased chemicals were used without further purification.

Characterization

NMR spectra were recorded on an Avance III HD NanoBay 400 MHz and Avance III HD 600 MHz *Bruker BioSpin GmbH* at 24 °C if not stated otherwise. ^{1}H- and ^{13}C-NMR chemical shifts (δ) were referenced to the solvent residual peak [C_6D_5H: δ(^{1}H) = 7.16 ppm] and the solvent peak [C_6D_6: δ(^{13}C) = 128.39 ppm], respectively. ^{29}Si-NMR were calibrated using tetramethylsilane [δ(^{29}Si) = 0.0 ppm] as an external standard, and the spectra were recorded using the INEPT pulse sequence. Spin-spin coupling constants (*J*) are reported in Hertz (Hz). Coupling patterns in the ^{1}H-NMR spectra are abbreviated as *s* (singlet), *br. s* (broadened singlet), *d* (doublet), *dd* (doublet of a doublet), *ddd* (doublet of a doublet of a doublet), *td* (triplet of a doublet) *p* (pentet), *m* (multiplet). The assignment of some signals was carried out through corresponding measurements of two-dimensional spectra (COSY, HSQC, HMBC).

Single crystal X-ray data were collected on a Bruker D8 Venture four-circle diffractometer from Bruker AXS GmbH, equipped with a Photon II CPAD detector. The measurements were carried out at 100 K using MoK_α radiation (λ = 0.71703 Å). Radiation source: IμS Mo microfocus source by Incoatex GmbH, equipped with HELIOS mirror optics and a single-hole collimator from Bruker AXS GmbH. The crystals were mounted with an SMZ1270 stereo microscope from Nikon Metrology GmbH. The crystals were mounted on MicroMounts, MicroLoops or MicroGrippers from MiTeGen in perfluoropolyalkylethers. *APEX v4.0*[20] in connection with *SAINT* (integration) and *SADABS* (adsorption correction) from *Bruker AXS GmbH* was used for the data collection.[21] The molecular structures were solved with *SHELXT*[22] and refined using *SHELXL*.[23] The final processing of structures was carried out with *OLEX*^{2}.[24] All non-hydrogen atoms were refined anisotropically, and all carbon-bound hydrogen atoms were placed in geometrically calculated positions according to a riding model.

Mass Spectrometry (GC/EI-MS coupling): Gas chromatograph from *Agilent* (model: 7890B); HP-5 MS capillary column from *Agilent* (length 30 m, ID 0.25 mm); carrier gas helium. EI-MS: Mass Selective Detector 5977 A from *Agilent* (electron impact ionization, 70 eV). The *m/z* values of the molecular ions and the selected fragment ions are based on the mass numbers of the isotopes with the highest natural abundance (^{1}H, ^{12}C, ^{14}N, ^{16}O, ^{28}Si).

Elemental Analysis: Instrument from the company *Elementar* (model: vario MICRO cube). The analytical data for a compound were reported as the mass percentages of the respective elements.

Quantum Mechanical Calculations: The calculations were performed using the program *Gaussian Version G09 Revision E.01*,[25] the molecular coordinates were generated using *GaussView Version 6.0.16*.[26] The ground state structures were optimized without any symmetry constraints. Subsequent frequency calculations confirmed the absence of imaginary frequencies for each minimum structure.

Syntheses

Preparation of the Racemic Methoxysilane rac-2[4]

Following a standard *Grignard* procedure,[12] 1-naphthylmagnesium bromide was prepared from 1-bromonaphthalene (202 g, 974 mmol) and magnesium turnings (23.7 g, 974 mmol) in THF (400 mL). The suspension was heated under reflux for 30 minutes. Then, methylphenyldimethoxysilane (162 g, 886 mmol) was added, and the solution was refluxed for additional 18 hours. The mixture was treated with NH_4Cl solution, and the aqueous phase was extracted with *n*-pentane. The combined organic phases were dried over Na_2SO_4, and the solvents were removed under reduced pressure. Fractional distillation (131 °C, 0.3 mbar) yielded the product (*rac*-**2**, 225.9 g, 811 mmol, 92 %) as a white solid. **^{1}H-NMR**: (400 MHz, C_6D_6, 24 °C) δ = 0.70 (s, 3 H; SiCH_3), 3.38 (s, 3 H; OCH_3), 7.12–7.18 (m, 3 H; $C_{Ar}H$, not baseline-separated because of C_6D_6), 7.19–7.22 (m, 2 H; $C_{Ar}H$), 7.30 (dd, $^3J_{HH}$ = 8.2 Hz, $^3J_{HH}$ = 6.8 Hz, 1 H;

$C_{Ar}H$), 7.63–7.67 (m, 3 H; $C_{Ar}H$), 7.87 (d, $^3J_{HH}=8.3$ Hz, 1 H; $C_{Ar}H$), (dd, $^3J_{HH}=6.8$ Hz, $^4J_{HH}=1.3$ Hz, 1 H; $C_{Ar}H$), 8.40–8.42 (m, 1 H; $C_{Ar}H$) ppm. **^{13}C{^{1}H}-NMR**: (126 MHz, C_6D_6, 24 °C) $\delta=-1.8$ (s; $SiCH_3$), 51.3 (s; OCH_2), 125.7, 126.3, 126.8, 128.6, 129.3, 129.6, 130.4, 131.5, (each s; $C_{Ar}H$), 134.4 (s; C_q), 134.6 (s; C_q) 135.0 (s; $C_{Ar}H$), 136.0 (s; $C_{Ar}H$), 137.4 (s; C_q), 138.1 (s; C_q) ppm. **^{29}Si{^{1}H}-NMR**: (60 MHz, C_6D_6, 24 °C) $\delta=0.1$ (s; *Si*) ppm. **GC/EI-MS**: [70 °C (2 min) with 20 °C min^{-1}–270 °C (10 min)] (70 eV, $t_R=13.10$ min). m/z (%): 278 (45) [M^+], 263 (100) [$M-CH_3^+$], 245 (3) [$M-OMe^+$], 233 (15) [$M-CH_3$,OMe^+], 202 (10) [NaphMeHSiOMe$^+$], 171 (5) [HNaphSi$^+$], 155 (13) [NaphSi$^+$], 121 (11) [PhMeSiH$^+$], 105 (7) [PhSi$^+$], 77 (3) [$C_6H_5^+$], 59 (3) [SiOMe]. **CHN**: $C_{18}H_{18}OSi$ (278.43 g mol^{-1}): calc. C 77.65 %, H 6.52 %; found C 77.9 %, H 6.5 %.

Preparation of the Menthoxysilanes (S_{Si})-3 and (R_{Si})-3 Diastereomers

rac-Methoxymethylphenylnaphthylsilane (*rac*-**2**, 72 g, 259 mmol) was reacted with (−)-menthol (40.5 g, 259 mmol) and KOH (0.36 g, 6.48 mmol) in toluene (300 mL) and heated under reflux for 6 hours. The resulting methanol was removed by distillation during the reaction. The reaction mixture was filtered, and the crude product was fractionally distilled (230 °C, 3.6·10^{-5} mbar). The product (both diastereomers) was obtained as a yellowish resin with a yield of 87.6 g (**3**, 218 mmol, 84 %). **GC/EI-MS**: [80 °C (1 min) with 10 °C min^{-1}–300 °C (7.5 min)] (70 eV, $t_R=19.93$ min). m/z (%): 402 (1) [M^+], 387 (2) [M–Me^+], 274 (64) [M–Naph,H^+], 247 (81) [M–OMen$^+$], 187 (16) [$C_{11}H_{11}OSi^+$], 169 (42) [$C_{11}H_9Si^+$], 137 (100) [$C_7H_9OSi^+$], 128 (32) [$C_{10}H_8^+$], 77 (3) [$C_6H_5^+$]. **CHN**: $C_{18}H_{18}OSi$ (402.24 g mol^{-1}): calc. C 80.54 %, H 8.51 %; found C 80.5 %, H 8.6 %.

Separation of (S_{Si})- and (R_{Si})-Diastereomers, (S_{Si})-3 and (R_{Si})-3, by Fractional Crystallization

The diastereomers (**3**, 80.8 g, 201 mmol) were separated by fractional crystallization from *n*-pentane. The diastereomeric mixture was dissolved in *n*-pentane (250 mL) and cooled to −80 °C for one week. The (S_{Si})-configured product crystallized out after three recrystallizations and was washed with cold *n*-pentane (3×30 mL) as well as separated, yielding 34.7 g [86.4 mmol, 43 %, 86 % of (S_{Si})-diastereomer] of the (S_{Si})-product as enantiomerically and diastereochemically pure (*d.r.* ≥ 99 : 1, *e.r.* ≥ 99 : 1). Afterwards, the *n*-pentane was removed from the mother liquor and the crude product was dissolved in diethyl ether (150 mL). The (R_{Si})-configured product remaining in solution was dissolved in diethyl ether and stored at −30 °C for approximately 2 weeks. The resulting crystals were washed with cold diethyl ether (3×30 mL), yielding 29.9 g [74.4 mmol, 37 %, 74 % of (R_{Si})-diastereomer].

Characterization of the (S_{Si})-Diastereomer (S_{Si})-3

^{1}H-NMR: (400 MHz, C_6D_6, 24 °C) $\delta=0.60$ (d, $^3J_{HH}=7.0$ Hz, 3 H; $CHCHCH_3$), 0.75 (d, $^3J_{HH}=6.5$ Hz, 3 H; $CHCH_3$), 0.72–0.76 (m, 2 H; $CHCHCH_2$ & $CHCH_2CH_2$, not baseline-separated because of $CHCH_3$), 0.81 (s, 3 H; $SiCH_3$), 0.89 (d, $^3J_{HH}=7.0$ Hz, 3 H; $CHCHCH_3$), 0.96–1.07 (m, 1 H; $CHCH_3$), 1.26 (td, $^2J_{HH}=12.1$ Hz, $^3J_{HH}=10.8$ Hz, 1 H; $OCHCH_2$), 1.39–1.52 [m, 3 H; $CHCH(CH_3)_2$ & $CHCH_2$ & $CHCH_2CH_2$], 1.96–2.01 (m, 1 H; $OCHCH_2$), 2.43–2.54 [m, 1 H; $CH(CH_3)_2$], 3.62 (td, $^2J_{HH}=10.2$ Hz, $^3J_{HH}=4.3$ Hz, 1H; *OCH*), 7.14–7.21 (m, 5 H; 5x $C_{ar}H$, not baseline-separated because of C_6D_6), 7.36 (dd, $^3J_{HH}=8.2$ Hz, $^3J_{HH}=6.8$ Hz, 1 H; $C_{ar}H$), 7.62–7.64 (m, 1 H; $C_{ar}H$), 7.71–7.75 (m, 3H; 3x $C_{ar}H$), 8.07 (dd, $^3J_{HH}=6.8$ Hz, $^3J_{HH}=1.3$ Hz, 1 H; $C_{ar}H$), 8.36 (dd, $^3J_{HH}=8.1$ Hz, $^4J_{HH}=1.4$ Hz, 1 H; $C_{ar}H$) ppm. **^{13}C{^{1}H}-NMR**: (101 MHz, $CDCl_3$, 24 °C) $\delta=0.0$ (s; $SiCH_3$), 16.3 (s; $CH(CH_3)_2$), 21.9 [s; $CH(CH_3)_2$], 22.8 (s; $CHCH_3$), 23.4 (s; $HCHCH_2$), 25.9 (s; OCHCHCH), 32.1 (s; CH_3CHCH_2), 35.1 (s; CH_3CHCH_2), 46.2 (s; $OCHCH_2$), 51.1 (s; OCHCH), 74.3 (s; *OCH*), 125.7 (s; $C_{Ar}H$), 126.1 (s; $C_{Ar}H$), 126.4 (s; $C_{Ar}H$), 129.5 (s; $C_{Ar}H$), 130.3 (s; $C_{Ar}H$), 131.4 (s; $C_{Ar}H$), 134.4 (s; C_q), 134.9 (s; $C_{Ar}H$), 135.7 (s; $C_{Ar}H$), 135.8 (s; C_q), 138.0 (s; C_q), 138.8 (s; C_q) ppm. **^{29}Si{^{1}H}-NMR**: (80 MHz, $CDCl_3$, 24 °C) $\delta=-5.4$ (s; *Si*) ppm. **GC/EI-MS**: [80 °C (1 min) with 10 °C min^{-1} −300 °C (7.5 min)] (70 eV, $t_R=19.91$ min). m/z (%): 402 (1) [M^+], 387 (2) [M–Me^+], 274 (74) [M–Naph,H^+], 247 (86) [M–OMen$^+$], 187 (19) [$C_{11}H_{11}OSi^+$], 169 (48) [$C_{11}H_9Si^+$], 137 (100) [$C_7H_9OSi^+$], 128 (31) [$C_{10}H_8^+$], 77 (3) [$C_6H_5^+$]. **CHN**: $C_{18}H_{18}OSi$ (402.24 g mol^{-1}): calc. C 80.54 %, H 8.51 %; found C 80.5 %, H 8.6 %. **Mp**: $T_{mp}=82.2-82.7$ °C. **Specific Rotation**: $[\alpha]_D^{20}=-29.316°$ (*n*-hexane).

Characterization of the (R_{Si})-Diastereomer (R_{Si})-3

^{1}H-NMR:(400 MHz, C_6D_6, 24 °C) $\delta=0.66$ (d, $^3J_{HH}=6.8$ Hz, 3 H; $CHCHCH_3$), 0.68 (d, $^3J_{HH}=6.5$ Hz, 3 H; $CHCH_3$), 0.73–0.78 (m, 2 H; $CHCHCH_2$ & $CHCH_2CH_2$), 0.82 (s, 3 H; $SiCH_3$), 0.96 (d, $^3J_{HH}=7.1$ Hz, 3 H; $CHCHCH_3$), 1.01–1.12 (m, 1 H; $CHCH_3$), 1.20 (td, $^2J_{HH}=12.1$ Hz, $^3J_{HH}=10.6$ Hz, 1 H; $OCHCH_2$), 1.39–1.52 [m, 3 H; $CHCH(CH_3)_2$ & $CHCH_2$ & $CHCH_2CH_2$], 1.94 (dt, $^2J_{HH}=12.1$ Hz, $^3J_{HH}=4.8$ Hz, 1 H; $OCHCH_2$), 2.58 (septd, $^3J_{HH}=7.0$ Hz, $^3J_{HH}=2.3$ Hz, 1 H; $CH(CH_3)_2$), 3.67 (td, 1H, $^3J_{HH}=10.1$ Hz, $^3J_{HH}=4.3$ Hz; *OCH*), 7.14–7.21 (m, 5 H; 5x $C_{ar}H$ not baseline-separated because of C_6D_6), 7.37 (dd, $^3J_{HH}=8.2$ Hz, $^3J_{HH}=6.8$ Hz, 1 H; $C_{ar}H$), 7.63–7.65 (m, 1H; $C_{ar}H$), 7.70–7.74 (m, 3H; 3x $C_{ar}H$), 8.10 (dd, $^3J_{HH}=6.8$ Hz, $^3J_{HH}=1.3$ Hz, 1 H; $C_{ar}H$), 8.39–8.42 (m, 1 H; $C_{ar}H$) ppm. **^{13}C{^{1}H}-NMR**: (101 MHz, $CDCl_3$, 24 °C) $\delta=-0.3$ (s; $SiCH_3$), 16.3 (s; $CH(CH_3)_2$), 22.0 [s; $CH(CH_3)_2$], 22.7 (s; $CHCH_3$), 23.4 (s; $HCHCH_2$), 26.0 (s; OCHCHCH), 32.1 (s; CH_3CHCH_2), 35.1 (s; CH_3CHCH_2), 45.8 (s; $OCHCH_2$), 51.2 (s; OCHCH), 74.2 (s; *OCH*), 125.7 (s; $C_{Ar}H$), 126.1 (s; $C_{Ar}H$), 126.4 (s; $C_{Ar}H$), 129.5 (s; $C_{Ar}H$), 130.3 (s; $C_{Ar}H$), 131.4 (s; $C_{Ar}H$), 134.4 (s; C_q), 135.0 (s; $C_{Ar}H$), 135.6 (s; $C_{Ar}H$), 136.0 (s; C_q), 138.0 (s; C_q), 138.6 (s; C_q) ppm. **^{29}Si{^{1}H}-NMR**: (80 MHz, $CDCl_3$, 24 °C) $\delta=-5.7$ (s; *Si*) ppm. **GC/EI-MS**: [80 °C (1 min) with 10 °C min^{-1} −300 °C (7.5 min)] (70 eV, $t_R=19.91$ min). m/z (%): 402 (1) [M^+], 387 (1) [M–Me^+], 274 (54) [M–Naph,H^+], 247 (74) [M–OMen$^+$], 187 (16) [$C_{11}H_{11}OSi^+$], 169 (45) [$C_{11}H_9Si^+$], 137 (100) [$C_7H_9OSi^+$], 128 (34) [$C_{10}H_8^+$], 77 (3) [$C_6H_5^+$]. **CHN**: $C_{18}H_{18}OSi$ (402.24 g mol^{-1}): calc. C 80.54 %, H 8.51 %; found C 80.4 %, H 8.4 %. **Mp**: $T_{mp}=62.5-62.8$ °C. **Specific Rotation**: $[\alpha]_D^{20}=-16.742°$ (*n*-hexane).

Acknowledgements

This research was funded by the Deutsche Forschungsgemeinschaft (DFG, German Research Foundation – 500221904. We would like thank the Fonds der Chemischen Industrie for a Kekulé-fellowship (K 208/39) as well as the Konrad-Adenauer-Stiftung for a KAS-PhD fellowship. The authors acknowledge the computing time provided on the Linux HPC cluster at Technische Universität Dortmund/TU Dortmund University (LiDO3), partially funded in the course of the Large-Scale Equipment Initiative by the Deutsche Forschungsgemeinschaft (DFG, German Research Foundation, project number 271512359). We wish Prof. Dr. Michael Veith all the best and good health on his 80th birthday! Open Access funding enabled and organized by Projekt DEAL.

Conflict of Interests

The authors declare no conflict of interest.

Data Availability Statement

The data that support the findings of this study are available in the supplementary material of this article.

Keywords: Silicon · Chirality · Silanes · Solid-state structures · X-ray diffraction

[1] a) F. Langenohl, J. Rösler, S. Zühlke, J.-L. Kirchhoff, C. Strohmann, *Chem. Eur. J.* **2023**, *29*, e202202935; b) X. Wang, C. Feng, J. Jiang, S. Maeda, K. Kubota, H. Ito, *Nat. Commun.* **2023**, *14*, 5561; c) Y. Wu, P. Wang, *Angew. Chem. Int. Ed.* **2022**, *61*, e202205382; d) Y. Wu, P. Wang, *Angew. Chem.* **2022**, *134*, e202205382.

[2] a) J. O. Bauer, C. Strohmann, *Eur. J. Inorg. Chem.* **2016**, *2016*, 2868; b) W.-E. Gan, Y.-S. Wu, B. Wu, C.-Y. Fang, J. Cao, Z. Xu, L.-W. Xu, *Angew. Chem. Int. Ed.* **2024**, *63*, e202317973; c) W.-E. Gan, Y.-S. Wu, B. Wu, C.-Y. Fang, J. Cao, Z. Xu, L.-W. Xu, *Angew. Chem.* **2024**, *136*, e202317973; d) T. Hu, C. Zhao, Y. Zhang, Y. Kuang, L. Gao, W. Wang, Z. Su, Z. Song, *Nat. Commun* **2023**, *14*, 4900.

[3] a) M. Oestreich, *Chem. Eur. J.* **2005**, *12*, 30; b) M. Oestreich, S. Rendler, *Angew. Chem. Int. Ed.* **2005**, *44*, 1661; c) M. Oestreich, S. Rendler, *Angew.Chem.* **2005**, *117*, 1688; d) T. Hayashi, K. Yamamoto, M. Kumada, *Tetrahedron Lett.* **1974**, *15*, 331.

[4] L. H. Sommer, C. L. Frye, G. A. Parker, K. W. Michael, *J. Am. Chem. Soc.* **1964**, *86*, 3271.

[5] a) L. H. Sommer, K. W. Michael, W. D. Korte, *J. Am. Chem. Soc.* **1963**, *85*, 3712; b) L. H. Sommer, P. G. Rodewald, *J. Am. Chem. Soc.* **1963**, *85*, 3898; c) L. H. Sommer, C. L. Frye, *J. Am. Chem. Soc.* **1959**, *81*, 1013; d) L. H. Sommer, J. E. Lyons, *J. Am. Chem. Soc.* **1969**, *91*, 7061; e) L. H. Sommer, *Angew. Chem. Int. Ed. Engl.* **1962**, *1*, 143; f) L. H. Sommer, *Angew. Chem.* **1962**, *74*, 176.

[6] a) R. J. P. Corriu, M. Henner, *J. Organomet. Chem.* **1974**, *74*, 1; b) R. J. P. Corriu, M. Henner, *J. Organomet. Chem.* **1980**, *198*, 231.

[7] a) T. Hayashi, K. Yamamoto, M. Kumada, *Tetrahedron Lett.* **1974**, *15*, 331; b) T. H. R. Tacke, *Silicon Chem.* **2002**, *2002*, 35.

[8] a) J. F. Klebe, H. Finkbeiner, *J. Am. Chem. Soc.* **1966**, *88*, 4740; b) J. F. Klebe, H. Finkbeiner, *J. Am. Chem. Soc.* **1968**, *90*, 7255; c) K. Kobayashi, T. Kato, M. Unno, S. Masuda, *Bull. Chem. Soc. Jpn.* **1997**, *70*, 1393; d) K. Kobayashi, T. Kato, S. Masuda, *Chem. Lett.* **1987**, *16*, 101; e) K. Igawa, N. Kokan, K. Tomooka, *Angew. Chem. Int. Ed.* **2010**, *49*, 728; f) K. Igawa, N. Kokan, K. Tomooka, *Angew. Chem.* **2010**, *122*, 740; g) K. Igawa, J. Takada, T. Shimono, K. Tomooka, *J. Am. Chem. Soc.* **2008**, *130*, 16132; h) A. Nakazaki, T. Nakai, K. Tomooka, *Angew. Chem. Int. Ed.* **2006**, *45*, 2235; i) A. Nakazaki, T. Nakai, K. Tomooka, *Angew. Chem.* **2006**, *118*, 2293; j) K. Tomooka, A. Nakazaki, T. Nakai, *J. Am. Chem. Soc.* **2000**, *122*, 408.

[9] a) M. Achternbosch, L. Zibula, J.-L. Kirchhoff, J. O. Bauer, C. Strohmann, *Inorg. Chem.* **2021**, *60*, 11562; b) E. R. Barth, A. Krupp, F. Langenohl, L. Brieger, C. Strohmann, *Chem Commun.* **2019**, *55*, 6882; c) S. G. Koller, J. O. Bauer, C. Strohmann, *Angew. Chem. Int. Ed.* **2017**, *56*, 7991; d) S. G. Koller, J. O. Bauer, C. Strohmann, *Angew. Chem.* **2017**, *129*, 8102; e) J. O. Bauer, C. Strohmann, *J. Am. Chem. Soc.* **2015**, *137*, 4304; f) J. O. Bauer, C. Strohmann, *Angew. Chem. Int. Ed.* **2014**, *53*, 8167; g) J. O. Bauer, C. Strohmann, *Angew. Chem.* **2014**, *126*, 8306; h) J. O. Bauer, C. Strohmann, *Angew. Chem. Int. Ed.* **2014**, *53*, 720; i) J. O. Bauer, C. Strohmann, *Angew. Chem.* **2014**, *126*, 738.

[10] a) R. K. Schmidt, H. F. T. Klare, R. Fröhlich, M. Oestreich, *Chem. Eur. J.* **2016**, *22*, 5376; b) K. Müther, R. Fröhlich, C. Mück-Lichtenfeld, S. Grimme, M. Oestreich, *J. Am. Chem. Soc* **2011**, *133*, 12442.

[11] a) M. Zhu, M. Oestreich, *ACS Catal.* **2023**, *13*, 10244; b) S. Chen, D. Mu, P.-L. Mai, J. Ke, Y. Li, C. He, *Nat. Commun.* **2021**, *12*, 1249; c) Y. Guo, M.-M. Liu, X. Zhu, L. Zhu, C. He, *Angew. Chem. Int. Ed.* **2021**, *60*, 13887; d) Y. Guo, M.-M. Liu, X. Zhu, L. Zhu, C. He, *Angew. Chem.* **2021**, *133*, 14006; e) B. Yang, W. Yang, Y. Guo, L. You, C. He, *Angew. Chem. Int. Ed.* **2020**, *59*, 22217; f) B. Yang, W. Yang, Y. Guo, L. You, C. He, *Angew. Chem.* **2020**, *132*, 22401; g) J. Zhu, S. Chen, C. He, *J. Am. Chem. Soc* **2021**, *143*, 5301; h) M. Oestreich, *Synlett* **2007**, *11*, 1629.

[12] V. Grignard, *Ann. Chim. Phys.* **1901**, *24*, 433.

[13] a) Y. Wu, P. Wang, *Angew. Chem. Int. Ed.* **2022**, *61*, e202205382; b) Y. Wu, P. Wang, *Angew. Chem.* **2022**, *134*, e202205382.

[14] H. D. Flack, *Acta Cryst.* **1983**, *A39*, 876.

[15] F. Kleemiss, O. V. Dolomanov, M. Bodensteiner, N. Peyerimhoff, L. Midgley, L. J. Bourhis, A. Genoni, L. A. Malaspina, D. Jayatilaka, J. L. Spencer, et al., *Chem. Sci.* **2020**, *12*, 1675.

[16] *This refers to data from the structure refinement using NoSpherA2. For both diastereomers, the NoSpherA2 refined data was uploaded to the CCDC. For (S_{Si})-* **3***: CCDC deposition number 2363296 [NoSpherA2 refined structure: 2367654] ; for (R_{Si})-***3***: CCDC deposition number 2363300 [NoSpherA2 refined structure: 2367642] .*

[17] F. H. Allen, O. Kennard, D. G. Watson, L. Brammer, A. G. Orpen, R. Taylor, *J. Chem Soc. Perkin Trans. II* **1987**, *12*, 1.

[18] M. A. Spackman, D. Jayatilaka, *CrystEngComm* **2009**, *11*, 19.

[19] P. R. Spackman, M. J. Turner, J. J. McKinnon, S. K. Wolff, D. J. Grimwood, D. Jayatilaka, M. A. Spackman, *J. Appl. Crystallogr.* **2021**, *54*, 1006.

[20] Bruker, APEX IV. Bruker AXS Inc., Madison, Wisconsin, USA **2021**.

[21] Bruker, *SADABS*. Bruker AXS Inc., Madison, Wisconsin, USA **2001**.

[22] G. M. Sheldrick, *Acta Cryst.* **2015**, *A71*, 3.

[23] G. M. Sheldrick, *Acta Cryst.* **2015**, *C71*, 3.

[24] O. V. Dolomanov, L. J. Bourhis, R. J. Gildea, J. A. K. Howard, H. Puschmann, *J. Appl. Crystallogr.* **2009**, *42*, 339.

[25] M. J. Frisch, G. W. Trucks, H. B. Schlegel, G. E. Scuseria, M. A. Robb, J. R. Cheeseman, G. Scalmani, V. Barone, G. A. Petersson, H. Nakatsuji, X. Li, M. Caricato, A. Marenich, J. Bloino, B. G. Janesko, R. Gomperts, B. Mennucci, H. P. Hratchian, J. V. Ortiz, A. F. Izmaylov, J. L. Sonnenberg, D. Williams-Young, F. Ding, F. Lipparini, F. Egidi, J. Goings, B. Peng, A. Petrone, T. Henderson, D. Ranasinghe, V. G. Zakrzewski, J. Gao, N. Rega, G. Zheng, W. Liang, M. Hada, M. Ehara, K. Toyota, R. Fukuda, J. Hasegawa, M. Ishida, T. Nakajima, Y. Honda, O. Kitao, H. Nakai, T. Vreven, K. Throssell, J. A. Montgomery, J. E. Peralta, F. Ogliaro, M. Bearpark, J. J. Heyd, E. Brothers, K. N. Kudin, V. N. Staroverov, T. Keith, R. Kobayashi, J. Normand, K. Raghavachari, A. Rendell, J. C. Burant, S. S. Iyengar, J. Tomasi, M. Cossi, J. M. Millam, M. Klene, C. Adamo, R. Cammi, J. W. Ochterski, R. L. Martin, K. Morokuma, O. Farkas, J. B. Foresman, D. J. Fox, Gaussian 09, Revision E.01, Gaussian, Inc., Wallingford CT (USA) **2016**.

[26] R. Dennington, T. A. Keith, J. M. Millam, *GaussView, Version 6.0.1.6*, Semichem Inc., Shawnee Mission, KS **2016**.

Manuscript received: July 4, 2024
Revised manuscript received: August 29, 2024
Accepted manuscript online: September 2, 2024

